Asymmetric architecture for heralded single-photon sources

Luca Mazzarella,[1,*] Francesco Ticozzi,[1,2] Alexander V. Sergienko,[3] Giuseppe Vallone,[1] and Paolo Villoresi[1]
[1]*Dipartimento di Ingegneria dell'Informazione, Università di Padova, via Gradenigo 6/B, I-35131 Padova, Italy*
[2]*Department of Physics and Astronomy, Dartmouth College, 6127 Wilder Laboratory, Hanover, New Hampshire 03755, USA*
[3]*Department of Electrical and Computer Engineering, Boston University, 8 Saint Mary's St., Boston, Massachusetts 02215, USA*
(Received 15 May 2013; published 27 August 2013)

Single-photon sources represent a fundamental building block for optical implementations of quantum information tasks ranging from basic tests of quantum physics to quantum communication and high-resolution quantum measurement. In this paper, in order to compare the effectiveness of different designs, we introduce a single-photon source performance index, based on the maximum probability of generating a single photon that still guarantees a given signal-to-noise ratio. We then investigate the performance of a multiplexed system based on asymmetric configuration of multiple heralded single-photon sources. The performance and scalability comparison with both currently existing multiple-source architectures and faint laser configurations reveals an advantage the proposed scheme offers in realistic scenarios. This analysis also provides insights on the potential of using such architectures for integrated implementation.

DOI: 10.1103/PhysRevA.88.023848 PACS number(s): 42.65.Lm, 03.67.−a, 42.50.Gy, 42.50.Ex

I. INTRODUCTION

The ideal source of single-photon quantum states is a key instrument for successful implementation of many exciting quantum information topics ranging from the schemes to probe foundations of quantum mechanics to super-resolution measurements and quantum metrology. Single-photon sources (SPSs) also represent a key resource for optical quantum computing and quantum communication. Optical quantum computers based on integrated photonic technology [1–4] can be built using linear optics and SPSs as shown by Knill, Laflamme, and Milburn [5]. In reality, specific designs that offer only some approximation of an ideal source can be achieved. For example, the current quantum key distribution (QKD) systems use weak laser pulses in place of single-photon sources [6–10] and a decoy state technique [11,12] to avoid the photon number splitting (PNS) attack [13] on the pulses containing more than one photon. The development of a scheme for producing true single-photon states would guarantee that all pulses contain one and only one photon thus allowing one to increase the key generation rate and to avoid any PNS attack. This challenging task has generated extensive efforts that lead to an appearance of multiple designs of heralded sources of single-photon states.

The single-photon source usually used in quantum information applications consists of a faint laser (FL), namely an attenuated and pulsed laser source.[1] For a coherent source the number of photons in each pulse can be modeled by a Poisson random variable. The probability of having k photon in each pulse is given by

$$\mathbb{P}_k = \frac{\mu^k}{k!} e^{-\mu}, \tag{1}$$

where μ is the mean number of photons in each pulse that depends on the power of the laser. Two indexes are usually employed in order to evaluate the output quality of the source: the *one-photon probability* $\mathbb{P}_1$ and the *signal-to-noise ratio*:

$$\mathrm{SNR} := \frac{\mathbb{P}_1}{1 - \mathbb{P}_0 - \mathbb{P}_1} = \frac{\mu}{e^{\mu} - 1 - \mu}. \tag{2}$$

The SNR is the ratio between the one-photon probability and the probability of having more than one photon in the output of the system. This index quantifies a critical quantity of the source: the number of multiple photons per pulse. In optical quantum computing this leads to errors whose effects are hard to detect and correct while in QKD it opens a possibility for PNS attacks. The main limitations of the FL source stems from the fact that μ is the only tunable parameter. This induces a trade-off: The value of μ that maximizes $\mathbb{P}_1$ is given by $\mu = 1$ and corresponds to a value of the one-photon probability of $e^{-1} \simeq 0.37$. However, for $\mu = 1$ the SNR is equal to $(e-2)^{-1} \simeq 1.39$, a value that is typically unacceptable for applications requiring a single-photon source. Since the SNR is unbounded for μ approaching zero, the mean photon number is usually kept sufficiently low in order to avoid multiphoton events, thus reducing also the overall probability of single-photon emission.

Several types of architectures with multiple heralded SPS have been proposed in order to overcome such natural limitations of the FL source. Photons are often generated in such devices by means of spontaneous parametric down-conversion (SPDC). In this nonlinear process an intense laser pump impinging on a nonlinear crystal leads to probabilistic emission of entangled pairs of photons (usually called signal and idler) into two different spatial modes, with their rate depending on the pump intensity, the nonlinear coefficient value, and on the length of the crystal. It is then possible to "herald" the presence of a photon in the signal mode by detecting the correlated twin photon in the idler mode. A heralded single-photon source based on SPDC with an overall heralding efficiency of 83% has been demonstrated very recently [14].

The scheme based on multiple heralded SPSs combined with the use of postselection has been originally proposed by Migdall [15] in order to enhance the probability of obtaining

*mazzarella@dei.unipd.it

[1]The use of pulsed driving electric fields allows one to limit the temporal interval when the photons are expected to exist thus reducing the impact of detector dark counts.

a single heralded photon. This implementation requires one to use the m-to-1 global switch. In the same work, the performance of the proposed scheme has been studied considering the finite detection efficiency. However, as pointed out in [16], an efficient implementation of such a device is not currently available, and it would be hardly scalable. To overcome these problems a symmetric scheme, employing a total of $m-1$ binary polarization-switching photon routers arranged in a modular tree structure has been proposed by Shapiro and Wong in [16]. They also considered the probability of emitting n photons taking into account the imperfectness or real detectors and optical switches. An experimental implementation of the scheme along with an essential discussion of its scalability has been pursued in [17] using four crystals. Recently, the analysis of multimode emission in SPDC used for SPS was carried out [18].

However, despite the recent theoretical and experimental improvement of single-photon sources, a thorough analysis of the performance of multiple heralded SPS in the presence of finite efficiencies, and their comparison with respect to a simple faint-laser source, is lacking: Nonetheless, it appears to be a crucial step in assessing their potential, especially in light of the experimental difficulties reported in [17]. In pursuing this analysis, we believe that one of the most delicate points consists in devising proper performance indexes, ensuring a fair comparison between different methods.

After reviewing the main ideas and theoretical results underlying the existing SPS architectures, we will present our results and performance analysis tools. In particular, the main results of our paper are the following:

(1) We introduce a performance index for single-photon sources to compare the effectiveness of different designs, i.e., the maximal single-photon probability achievable while guaranteeing a given signal-to-noise ratio. This index represents a fair way to compare the performances of general single-photon sources, regardless of the architecture or main principles these may rely on.

(2) We demonstrate that the heralded symmetric architecture proposed in [16] suffers from a scalability problem: Increasing the number of crystals beyond a certain value, depending on the detection efficiency and the router transmissivity, is detrimental to the performance. No previous analysis demonstrated this problem.

(3) We propose an asymmetric heralded scheme, and demonstrated that its performances always improve by increasing the numbers of crystals.

(4) We develop a comprehensive comparison between the symmetric and asymmetric configurations demonstrating that the asymmetric architecture outperforms the symmetric scheme in a large and, most importantly, experimentally relevant region of the parameter space.

II. PERFORMANCE INDEX FOR SINGLE-PHOTON SOURCES

In this section we present the key ideas underlying a class of source architectures that outperform the FL scheme and introduce a performance index for comparing different single-photon sources.

A. Multiple sources and the advantage of postselection

The building block of such architectures is represented by the so-called heralded source (HS). The HS exploits the SPDC effect on a nonlinear crystal pumped with a strong coherent field, which leads (with a certain probability) to the simultaneous generation of a pair (or more pairs) of photons: If the duration of the pulse (Δt_p) is much shorter than the measurement time interval (ΔT), but much greater than the reciprocal of the phase-matching bandwidth $\Delta\omega$, i.e., $\Delta T \gg \Delta t_p \gg 1/\Delta\omega$, the statistics of the pairs is still Poissonian [16]. One photon (the idler) of the pair is then fed to a photon detector, while the other photon is used as signal. The HS can be employed in multiple crystal strategies that outperform the FL by exploiting the parallel use of HS units and postselection strategies: Intuitively, the advantage of using a scheme exploiting a parallel implementation lies in the fact that the intensity of the pump of each crystal can be kept low, suppressing thus the multiphotons events, while keeping an acceptable production rate of single photons.

Let us assume for now to employ ideal detectors in order to illustrate in a simple setting the potential advantages offered by this system. The case of finite efficiency will be discussed later in this section. We here consider standard single-photon APD detectors only able to discriminate between the case of no incident photons and the case in which photons are detected, without resolving their number. When a detector is hit by the photons, it returns an electric signal (*trigger*), which indicates the presence of at least one photon in the signal channel.

Let us consider a multiple crystals heralded source architecture with postselection (MHPS) built as follows (see Fig. 1): an array of m HS units, labeled with index $i = 1, \ldots, m$, and each one simultaneously fed with a laser pulse with intensity such that the mean number of produced pairs is $\tilde{\mu}$. For each HS unit, the idler photon is used as a trigger and the other is injected into an optical switch. The optical switch selects, depending on the triggers, which signal channel must be routed to the global output.

As first proposed in [15] we use the following strategy for the switch: The output signal is taken from the first source (starting from $i = 1$) that triggers (thus indicating the presence of at least a photon in the channel). If all the detectors do not fire there are no photons in the signal channel. It is worth noting that the precise structure of the switch is not important

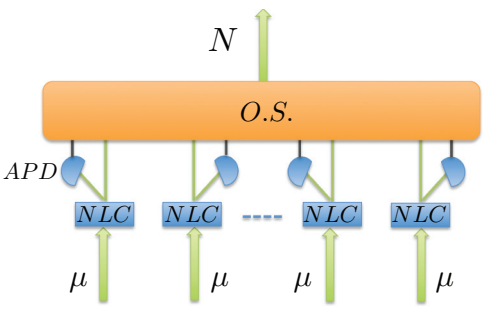

FIG. 1. (Color online) Schematic of the MHPS scheme. The rectangles labeled with NLC represent the nonlinear crystals, the detectors are labeled with APD, and the rectangle labeled with $O.S.$ represents the optical switch.

in this ideal situation. In fact, any switch that selects a channel when at least the corresponding HS has triggered could be used without altering the performances. We will see in the next section how different selection rules affect crucially the performances once the nonideal situation is kept into account.

The probability of having n photons in the global output of the MHPS is given by (see Appendix A for its derivation)

$$\mathbb{P}_n = \frac{\tilde{\mu}^n}{n!} e^{-\tilde{\mu}} \frac{1 - e^{-m\tilde{\mu}}}{1 - e^{-\tilde{\mu}}} (1 - \delta_n) + \delta_n e^{-m\tilde{\mu}}. \tag{3}$$

In the previous expression δ_n is the Kronecker Delta ($\delta_0 = 1$ and $\delta_{n\neq 0} = 0$).

In particular, the single-photon emission probability and the SNR are given by

$$\mathbb{P}_1 = \tilde{\mu} e^{-\tilde{\mu}} \frac{1 - e^{-m\tilde{\mu}}}{1 - e^{-\tilde{\mu}}}, \quad \mathrm{SNR} = \frac{\tilde{\mu}}{e^{\tilde{\mu}} - 1 - \tilde{\mu}}. \tag{4}$$

Notice that, when $\tilde{\mu} = \mu$, the signal-to-noise ratio is equal to the SNR of the faint laser, while the single-photon probability $\mathbb{P}_1$ is always larger.

B. Proposed performance index

As we have stated previously, in many applications it is crucial to be able to rely on a threshold value for the SNR. With this in mind, we propose the following method to compare different single-photon sources: we fix a threshold value for the acceptable SNR, Θ, and by varying μ we compute the maximum of the one-photon probability $\mathbb{P}_1$ provided that the SNR has a greater or equal value than Θ, namely,

$$\overline{\mathbb{P}}_1(\Theta) = \max_{\mu,\ \mathrm{SNR}\geqslant\Theta} \mathbb{P}_1(\mu). \tag{5}$$

From now on, $\overline{\mathbb{P}}_1$ always indicates this optimized probability with the SNR constraint. We note that, since the value of the SNR in Eq. (4) is between 0 and $+\infty$, by choosing the appropriate value of μ, any value of the SNR can be achieved. In Fig. 2 we show the maximized one-photon probabilities of different MHPS schemes in the function of the guaranteed SNR.

The benefits of the MHPS with respect to the FL are apparent: At any fixed SNR level, it is possible to obtain a higher value of the one-photon probability with MHPS. This is because of the postselection procedure, that can turn (with a certain probability) events in which more than one detectors trigger at the same time into an event that corresponds to a one-photon output *by blocking the output of all the HS units but one*.

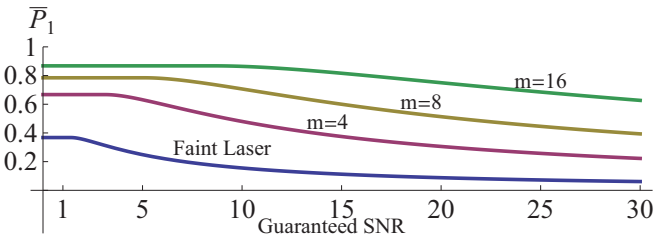

FIG. 2. (Color online) One-photon probability $\overline{\mathbb{P}}_1$ for the faint laser and the MHPS scheme, with $m = 4, 8$, and 16 in the function of the guaranteed SNR.

C. Finite efficiency and symmetric modular architecture

Any discussion regarding the physical implementations would be vain without taking into account the realistic efficiencies in detection and routing of the produced photons. An actual detector, in fact, is subject to losses whose effects are usually described by introducing a parameter $0 \leqslant \eta \leqslant 1$, called *detection efficiency*, that represents the probability of detecting an incident photon. This parameter takes into account also the collection efficiency due to the phase matching relation.

Physical implementation of postselection rules are subject to losses as well. The efficiency in transmission is modeled with a parameter $0 \leqslant \gamma \leqslant 1$, called *transmissivity*, that represents the probability of transmission for a photon through the router. It is important to note that this limited efficiency is referred only to the transmission of the photons: For what concerns the transmission of the electrical signal we are always going to assume that, once a trigger happens, it is transmitted until the end of the transmission chain without errors.

We remark that, in order to consider the role of a finite transmissivity, it is key to specify the particular routing/switching architecture that is being considered, since the potential gain with respect to an FL (without the routing inefficiencies) will in general depend on it. This is not the case in the ideal scheme described in the previous section.

In what follows we are going to briefly review a modular architecture, proposed in [16], that employs binary photon routers (2-to-1). The m-HS units are arranged as shown in Fig. 3: The outputs of the first stage are fed into the second stage's routers and so on, until the end of the transmission chain. This architecture can be clearly realized only for $m = 2^k$, with $k \in \mathbb{N}$. It is worth noting that any successfully transmitted photons have to pass trough $k = \log_2 m$ routers. We will call this scheme symmetric multiple-crystals heralded source with postselection (SMHPS). Each binary router selects the right signal channel only when the left HS has not triggered and the right HS has triggered: In all other cases it selects the left signal channel. The overall effect of the routers is that, if more than one detectors fire, the channel routed to the end of the chain is the one coming from the crystal corresponding to the lowest i. Differently from the scheme proposed in [16], if

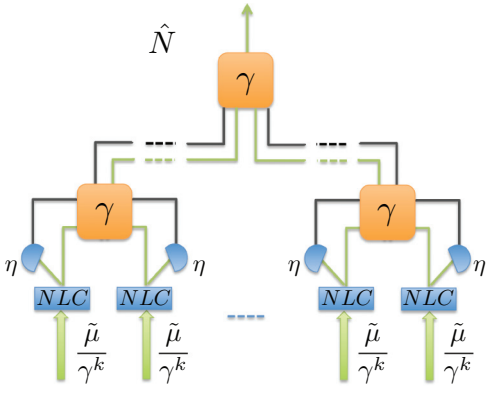

FIG. 3. (Color online) Schematic of the SMHPS scheme proposed in [16]. The rectangles labeled with NLC represent the nonlinear crystals, the detectors are labeled with η and the squares, labeled with γ, are the photon routers.

no detectors fire, the first channel is routed to the end: In fact, even in this case, there is some probability, due to detection inefficiency, that a photon is generated and it is convenient to route one channel to the end. With this choice the SMHPS always outperforms the faint laser.

Let us consider that each HS produces a mean number of pair given by $\widetilde{\mu}/\gamma^k$: We use this convention to compensate the γ^k factor arising from the binary switch transmission. As shown in Appendix A, the probability of having n photons in the final output is

$$\mathbb{P}_n^S = \frac{[(1-\eta)\widetilde{\mu}]^n e^{-(1-\eta)\widetilde{\mu}}}{n!} e^{-\eta\widetilde{\mu}\frac{\gamma^k}{\gamma^k}} + \frac{\widetilde{\mu}^n e^{-\widetilde{\mu}}}{n!} \frac{1-(1-\eta)^n e^{-\eta(\frac{1}{\gamma^k}-1)\widetilde{\mu}}}{1-e^{-\eta\frac{\widetilde{\mu}}{\gamma^k}}} \left(1-e^{-\eta\widetilde{\mu}\frac{\gamma^k}{\gamma^k}}\right). \quad (6)$$

The first term in the previous sum accounts for the probability of having some photons in the output when no detector fired. We notice that, in the ideal case of $\eta = \gamma = 1$ we obtain Eq. (3), while in the limiting case of null detection efficiency η, we obtain the faint laser source with mean photon number $\widetilde{\mu}$: The latter property is related to the choice of routing the first channel to the global output when no detectors fire. We will postpone the performances comparison of SMHPS with the FL in Sec. IV.

III. PROPOSED ASYMMETRIC ARCHITECTURE

In all the previous works, it was assumed that all the crystals in the symmetric architecture were driven with the same intensity. In Appendix B we will prove that this symmetric choice represents a suboptimal case for the one photon probability. In fact, even if the architecture is symmetric, an asymmetry comes from the binary switcher: The left source is initially checked and, only if this source doesn't trigger, the switch considers the right source. This asymmetry can be turned in a resource to increase the one-photon output probability: We here propose an asymmetric scheme which is scalable in the number of crystals and that performs better than the SMHPS in many situations of experimental interest, still being suboptimal in exploiting the available resources.

Let us suppose having an array of the m-HS system arranged asymmetrically as Fig. 4. This scheme also employs the same kind of binary switches but the multiplexing is performed in a different way with respect to the symmetric configuration: The output of an m-source block is obtained by combining the output of a block with m-1 sources with the output of an mth source. An evident advantage with respect to the symmetric configuration is the possibility of adding a single HS without the constraint of having 2^k crystals.

In this new configuration each successfully transmitted photon passes through a number of photon routers k_i that depends on which crystal it has been created from:

$$k_i = \begin{cases} i, & \text{if} \quad i \leqslant m-1 \\ m-1, & \text{if} \quad i = m. \end{cases} \quad (7)$$

Since each channel is subjected to a different attenuation, we again compensate the different absorption rates by choosing μ_i (the mean number of the generated pair of the ith crystal)

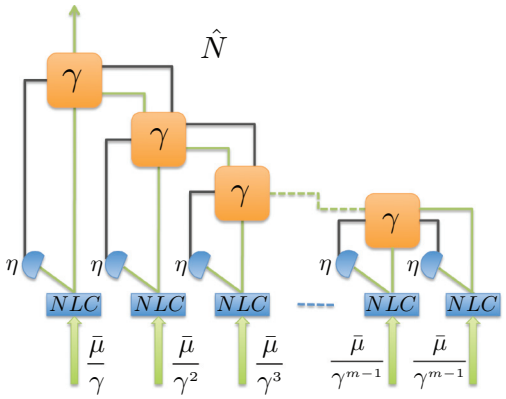

FIG. 4. (Color online) Schematics of the AMHPS. Notice that each crystal is fed with different intensities to compensate for the different absorption rate of different channels. The rectangles labeled with NLC represent the nonlinear crystals, the detectors are labeled with η, and the squares, labeled with γ, are the photon routers.

as

$$\mu_i = \frac{\bar{\mu}}{\gamma^{k_i}}, \quad i = 1, \ldots, m. \quad (8)$$

This choice is still suboptimal (a full optimization requires the numerical finding of the μ_i values, in the function of m, γ, and η, that maximize $\overline{\mathbb{P}}_1$) but is sufficient to outperform the SMHPS in many situations of experimental interest. To further improve the performances, an optimization over the different μ_i should be performed. As an example, we show in Appendix B that in the ideal case case of $\eta = \gamma = 1$ the one-photon probability can be improved by using optimized pump parameters. However, the optimization with imperfect efficiency and transmission cannot be performed analytically.

This multiplexing architecture is therefore asymmetric and will be denoted with AMHPS, to highlight the differences with the SMHPS scheme. It is worth noting that both the symmetric and the asymmetric architecture with the same number m of crystals, require the same number (m-1) of detectors and routers. With each binary switch configured as before, if two or more channels are heralded, the one that needs to pass through less routers is selected and routed to the end of the chain, thereby decreasing the probability of absorption. Again, if no detector fires, the first channel is routed to the end. Moreover, the different delay lines should be carefully adjusted such that each source would produce a final output photon at the same time.

As shown in Appendix A, the probability of emitting n photons for the AMHPS is given by

$$\mathbb{P}_n^A = \frac{[(1-\eta)\bar{\mu}]^n e^{-(1-\eta)\bar{\mu}}}{n!} e^{-\eta\bar{\mu}\frac{(2-\gamma)\gamma^{1-m}-1}{1-\gamma}} + \frac{\bar{\mu}^n e^{-\bar{\mu}}}{n!} \sum_{i=1}^{m} e^{-\eta\bar{\mu}\frac{\gamma^{1-i}-1}{1-\gamma}} \left[1-(1-\eta)^n e^{\eta\bar{\mu}} e^{-\frac{\eta\bar{\mu}}{\gamma^{k_i}}}\right]. \quad (9)$$

It worth noting that, by using the compensation proposed in (8), the dependence of the one-photon probability on the intensities is reduced to a single variable, i.e., $\bar{\mu}$. Moreover, when $\gamma \to 1$, the value of $\mathbb{P}_n^A$ for the asymmetric scheme coincides with the values $\mathbb{P}_n^S$ [Eq. (6)] of the symmetric scheme for any η. Again,

in the limiting case of $\eta \to 0$, we obtain the faint laser source with mean photon number $\bar{\mu}$.

In the next section we are going to confront the FL, the SMHPS, and the AMHPS.

IV. PERFORMANCE COMPARISON

This section is devoted to the comparison of the FL, the SMHPS, and the AMHPS by means of numerical considerations. We will use the performance index previously defined, namely the maximum of the one-photon probability $\mathbb{P}_1$ provided that the SNR has a greater or equal value than Θ:

$$\overline{\mathbb{P}}_1(\eta,\gamma,\Theta) = \max_{\mu,\mathrm{SNR}\geqslant\Theta} \mathbb{P}_1(\mu,\eta,\gamma). \tag{10}$$

Similarly to the ideal case, since $\lim_{\mu\to 0}\mathrm{SNR} = +\infty$ and $\lim_{\mu\to+\infty}\mathrm{SNR} = 0$ for both the symmetric and the asymmetric scheme, by choosing the appropriate value of μ, any value of the SNR can be achieved. Notice that, once the number of crystals and the SNR threshold are fixed, the above quantity depends only on (η,γ).

A. Scalability of the schemes for finite efficiencies

We first discuss the scalability features of the architectures with respect to the total number of crystals. In Figs. 5 and 6 we plotted the values of $\overline{\mathbb{P}}_1^A$ and $\overline{\mathbb{P}}_1^S$ versus the number of crystals m, ranging from 2 to 256 for different pairs of (η,γ) and for threshold SNR given by $\Theta = 10$.

For what concern the AMHPS it is apparent that, for all the considered pairs of (η,γ), the one-photon probability increases until it reaches an asymptotic value (the dependence of this value on γ and η is nontrivial). This fact implies that, once the detection efficiency and the transmissivity are fixed, there is a threshold value on the number of crystals above which there is no further improvement in the performances of the scheme. It is worth noting that for experimental realistic parameters, i.e., $\gamma \lesssim 0.5$, the asymptotic performances are practically already reached for $m = 8$.

For what it concerns the SMHPS, after an initial transient, the one-photon probability starts to decrease (apart from the ideal case of $\gamma = 1$). We have analytically shown that, excluding the $\gamma = 1$ case, in the limit of an infinite number of crystals ($m \to +\infty$) the one-photon probability of the symmetric scheme approaches the one-photon probability of the faint laser when the pump parameters are chosen

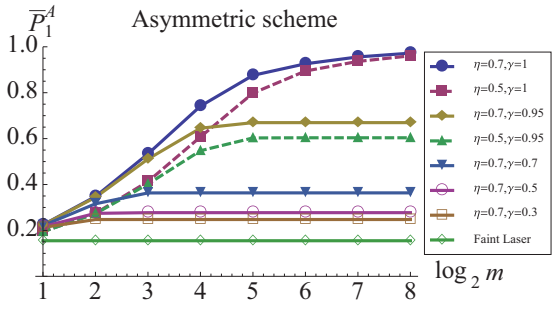

FIG. 5. (Color online) One-photon probability for the AMHPS with $\Theta = 10$ and $m \in \{2,\ldots,256\}$ and various pairs of (η,γ). We also report the corresponding $\overline{\mathbb{P}}_1 = 0.155$ of the faint laser.

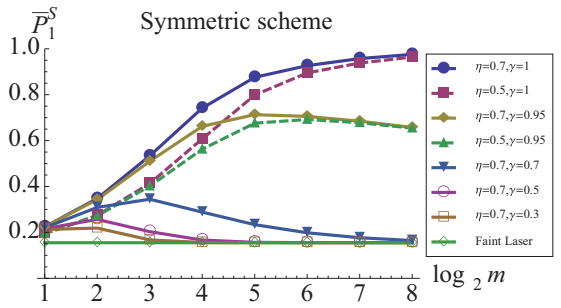

FIG. 6. (Color online) One-photon probability for the SMHPS with $\Theta = 10$ and $m \in \{2,\ldots,256\}$ and various pairs of (η,γ). We also report the corresponding $\overline{\mathbb{P}}_1 = 0.155$ of the faint laser.

in order to have asymptotically the same SNR (as can be seen in Fig. 6). The result is demonstrated in Appendix C. This property implies that the performances of symmetric architecture degrade if we increase too much the number m of crystals and a "fine tuning" of m should be used in function of η and γ to optimize $\overline{\mathbb{P}}_1^S$. Note that only if the parameters η and γ are perfectly know the optimization on the number of crystals can be performed exactly. The asymmetric scheme, on the other side, is always improving when the number of crystals is increased: From this point of view it is more "robust" than the symmetric scheme, since it does not require the precise knowledge of η and γ.

Let us try to give a motivation for this counterintuitive behavior: As we have mention above, in the SMHPS each successfully transmitted photon has to pass through $\log_2 m$ routers; increase the number of crystal means also to increase the absorption rate the photons are subjected to. Thus for this geometry architecture the benefits deriving from the increase of the number of crystals do not compensate the increase in the absorption rate. On the contrary, as we have mention above, in the AMHPS are most likely to be selected those channels whose photons have to pass through less routers in order to reach the global output leading, on average, to a lower absorption rate.

Summarizing, there are some benefits for the SMHPS in increasing the number of crystals but only up to a certain number, depending on the detection efficiency and transmissivity. Anyway increasing further the number of crystals will lead to poorer and poorer performances.

The AMHPS offers significant benefits in increase the number of crystals until a certain number depending on the detection efficiency and transmissivity; once the threshold is reached, increasing further the number of crystal will left the performances unchanged. Finally, we remark that since the two methods adopt the same post-selection rules, the gap in the performances arises form the different architecture geometries that is responsible for the different distribution of the routers.

Before closing this section, let us briefly review and discuss the scalability analysis proposed in [15]. In that paper, in order to evaluate the advantages of a scheme with respect to the FL, the *gain*, namely the ratio G between the one-photon probability of having one photon in the output of the SMHPS and the probability of producing one photon with the FL, is considered. It is worth remarking that in [15] the one-photon

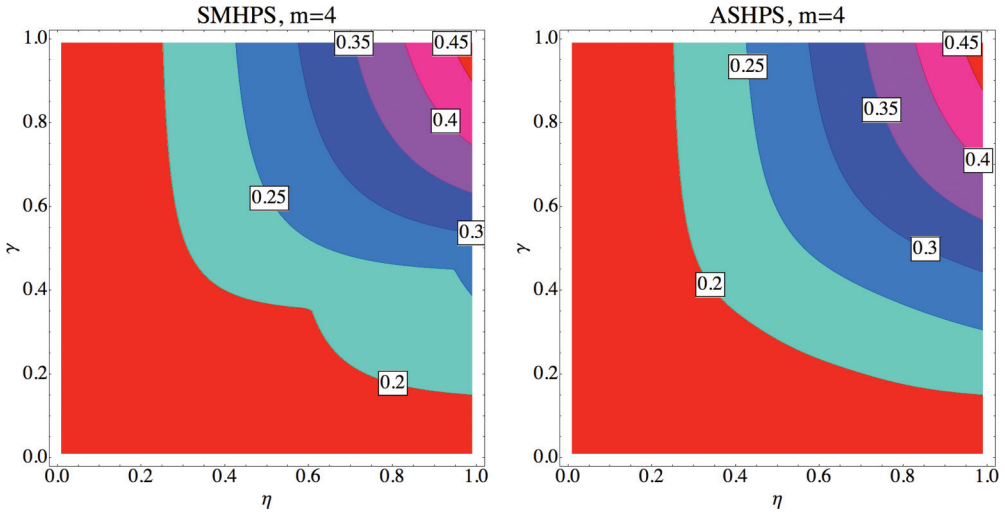

FIG. 7. (Color online) Contours of the one-photon probability for the SMHPS (left) and the AMHPS (right) with guaranteed SNR, $\Theta = 10$, and $m = 4$. For the symmetric architecture, for each (η,γ) we choose the number of crystals $m' \leqslant m$ that maximize $\overline{\mathbb{P}}_1$. $\overline{\mathbb{P}}_1$ is always above the value of the one-photon probability (given by 0.155) of the FL with guaranteed SNR equal to 10. In the SMHPS, the contour lines are not always smooth due to the changes in the m' value.

probability for the proposed scheme is computed neglecting both detection and transmission inefficiencies: In this ideal case, it turns out that both the scheme and the FL have the same SNR provided that the intensity with which the HS units are fed is equal to the intensity of the FL. In order to analyze the scalability taking into account the absorption due to the routing chain, they propose to consider the asymptotic behavior of the product $\gamma^k G$, thus comparing the benefits of a growing multicrystal architecture to the increase in the absorption rate due to the longer routing chain. As a result of this analysis, we have that the advantage of the SMHPS is maintained (i.e., $\lim_{k\to\infty} \gamma^k G > 1$) if $\gamma \geqslant 1/2$.

In order to perform a similar analysis we should compare the asymptotic behavior, in the limit of an infinite number of crystals, of the rate between the one-photon probability for the SMHPS, Eq. (6), with the probability of producing one photon with the FL, for the same SNR. As shown in Appendix C, in the $k \to \infty$ limit the SNR of the faint laser with intensity μ is equal to the SNR of the SMHPS with $\tilde{\mu} = \mu$ (the number of crystal is $m = 2^k$). Moreover, as explained previously, in order to avoid infinite power we need to rescale the pump power (for both the FL and the SMHPS) with the number of crystals, $\mu \to \mu/2^k$. The gain we obtain is given by

$$\widetilde{G} = \frac{1 - e^{-\frac{1-\gamma^k}{(2\gamma)^k}\eta\mu}(1-\eta) - e^{-\frac{\eta\mu}{\gamma^k}}\left[1 - e^{\frac{\eta\mu}{2^k}}(1-\eta)\right]}{1 - e^{-\frac{\eta\mu}{(2\gamma)^k}}}. \qquad (11)$$

In the infinite k limit, the gain $\widetilde{G}$ is greater than 1 for $\gamma \geqslant \frac{1}{2}$ (and is actually divergent for $\gamma > 1/2$) as found in [15]. However, in the rescaled pump power case, the one-photon probability of the SMHPS tends asymptotically to zero and the gain does not seem the proper index to evaluate the absolute performance of a scheme. In fact, despite exhibiting an advantage with respect to the FL, $\mathbb{P}_1$ is asymptotically zero in both cases (on the other hand, as already said, without the rescaling $\mu \to \mu/2^k$, the single-photon probability of the SMHPS and of the FL coincide in the large k limit, and the gain is always 1).

This means that, with finite transmissivity, not only increasing the number of crystal beyond a certain value does not bring any advantage, but it is *actually detrimental* to the SMHPS scheme performance. On the other hand, the AMHPS scheme is "robust" with respect to implementations with large numbers of crystals, as it is clearly shown in Fig. 5.

B. Comparison between AMHPS and SMHPS

We here compare the performances of the AMHPS and the SMHPS by fixing the guaranteed SNR and the number of crystals m. However, in order to obtain a fair comparison we analyze the asymmetric scheme with m crystals with the symmetric scheme with $m' \leqslant m$ crystals: In fact, as we have previously shown, the performance of the symmetric scheme does not always improve when the number of crystals is increased. Thus, for each (η,γ), the asymmetric scheme with m crystals must be compared with the symmetric scheme with m' crystals, where $m' \leqslant m$ is chosen in order to maximize $\overline{\mathbb{P}}_1$. In Figs. 7 and 8 we displayed the contours plot of $\overline{\mathbb{P}}_1$ for the AMHPS and the SMHPS with SNR threshold given by $\Theta = 10$ and $m = 4$ and 8, respectively. When $\Theta = 10$ the one-photon probability $\overline{\mathbb{P}}_1^{\mathrm{FL}}$ of the faint laser is given by 0.155. We can see that both the AMHPS and the SMHPS always outperform the FL in the plane (η,γ). As expected, the best performances are reached for high values of both the detection efficiency and the transmissivity: Furthermore in this limit the two methods are comparable since for $\eta \to 1$ and $\gamma \to 1$ they both tend to the ideal situation of the MHPS.

We can also define

$$\Delta(\eta,\gamma,\Theta) := 100\frac{\overline{\mathbb{P}}_1^A - \overline{\mathbb{P}}_1^S}{\overline{\mathbb{P}}_1^S}, \qquad (12)$$

as the percentage differences between the two optimized single-photon probabilities. In Fig. 9 we shown the contour of Δ for an SNR equal to 10 and $m = 4$ and 32. The AMHPS

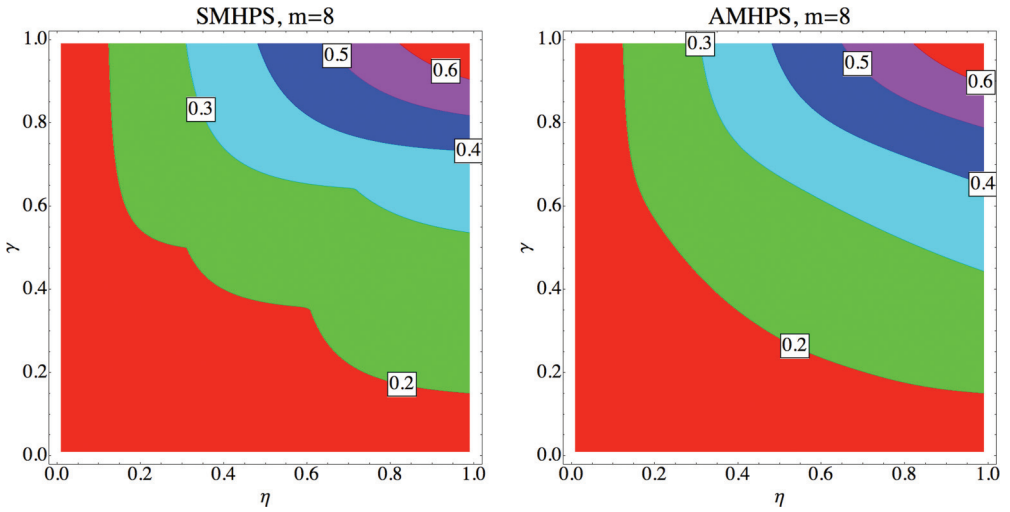

FIG. 8. (Color online) Contours of the one-photon probability for the SMHPS (left) and the AMHPS (right) with guaranteed SNR, $\Theta = 10$, and $m = 8$. For the symmetric architecture, for each (η,γ) we choose the number of crystals $m' \leqslant m$ that maximize $\overline{\mathbb{P}}_1$. $\overline{\mathbb{P}}_1$ is always above the value of the one-photon probability (given by 0.155) of the FL with guaranteed SNR equal to 10. In the SMHPS, the contour lines are not always smooth due to the changes in the m' value.

outperforms the SMHPS in a vast portion of the plane (η,γ). Anyway, the advantage of the AMHPS in more realistic situations is apparent, especially in the area where $\gamma \approx 0.5$ and the detection efficiency is higher than 0.5, the AMHPS outperforms the SMHPS.

Let us now focus on the timing performance of the two schemes. The difference between the symmetric and asymmetric scheme, apart from the value of $\mathbb{P}_1$, is the delay between the input pump pulse and the output photon. Let us define the delay between the emission of a photon from the crystal or from a router to the subsequent router by Δt, and assume for the sake of simplicity this is the same at every step, and for both architectures. In the symmetric configuration with 2^k crystals the output photon will come out with a delay $k\Delta t$ with respect to the pump pulse. In the asymmetric configuration with $m = 2^k$ crystals the output photon will come out with delay $2^k\Delta t$. However, these delays are fixed and well known, hence they do not lead to any inefficiency. Moreover, if we consider a train of pump pulses, such a difference has no practical effect other than an initial short delay: At the steady state both the symmetric and asymmetric architectures produce single photons with the same repetition rate. We note also that, with fast switches, delay Δt could be of the order of 10 ns: Even with $m = 10^8$ crystals, after 1 s the asymmetric source would have reached its steady state, corresponding to the same repetition rate of the symmetric architecture.

V. EXPERIMENTAL FEASIBILITY AND CONCLUSIONS

Let us now discuss a possible experimental realization of the proposed SPS configuration. Nowadays, integrated devices represent the best resource to achieve high efficiency of the

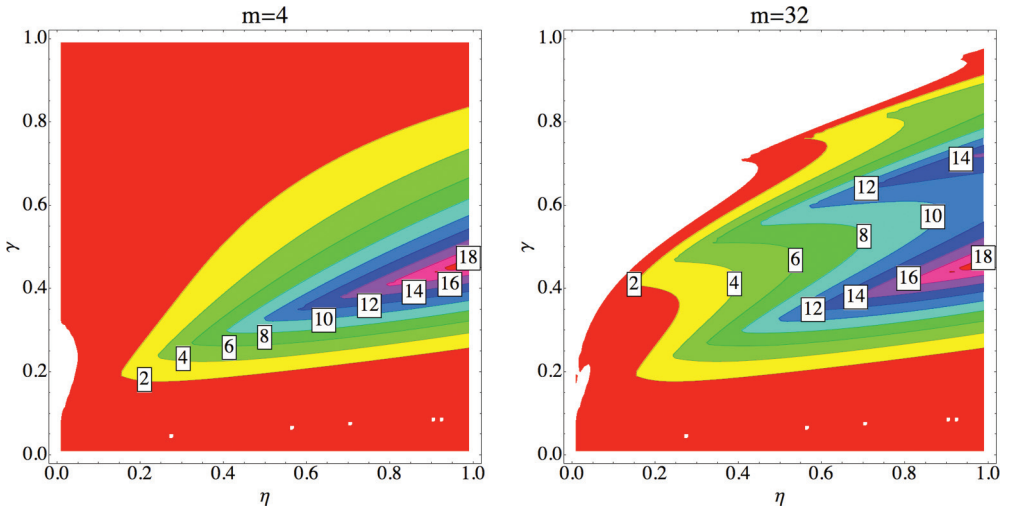

FIG. 9. (Color online) Contours of the percentage differences (12) with guaranteed SNR, $\Theta = 10$, and $m = 4$ (left) or $m = 32$ (right). Again, for the symmetric architecture, for each (η,γ) we choose the number of crystals $m' \leqslant m$ that maximize $\overline{\mathbb{P}}_1$. In the white area the SMHPS is performing better than the AMHPS.

SPDC process and ensure good coupling into single-mode fibers (for a review on integrated source see [19]). It is possible to use nondegenerate collinear phase matching and a dichroic beam splitter (or alternatively using a counterpropagating mode source [20]) in order to separate the two beams. For instance, it was recently reported the possibility of heralding single telecom photons at 4.4 MHz rate with 45% heralding efficiency [21]. Moreover, to efficiently detect the triggered photon, high efficient transition-edge sensors (TES) can be used: A heralding efficiency of $\eta \sim 62\%$ has been recently reported by using TES [22], while the 810-nm single-photon heralded source with 83% heralding efficiency has been shown in [14] (see also [23] for a review on single-photon detectors). Regarding the optical switch, a 2×2 silicon electro-optic switch with a broad bandwidth (60 nm), an ultrafast speed (6 ns), and a transmission of $\gamma \sim 50\%$ has been reported [24]; other modulators otherwise allow lower losses at the cost of a reduced working spectrum [25]. As shown in Fig. 7, with these values of η and γ, the asymmetric scheme is more performant than the symmetric one.

In conclusion we have proposed an asymmetric architecture for the multiplexed heralded single-photon source and we have compared it with the symmetric version proposed in [16] and with the faint laser source by using a performance index $\overline{\mathbb{P}}_1$ we introduced. We have proven that the asymmetric architecture outperform the symmetric scheme in a vast region of the parameter space (η,γ) and both outperform the FL for any values of γ and η. We have also demonstrated that, in the large number of crystal limit and by considering a fixed SNR, the symmetric configuration is asymptotically equivalent to the faint laser for any $\gamma \neq 1$, while for the asymmetric scheme the one-photon probability increases until it reaches an asymptotic value dependent on γ and η. This implies that the symmetric architecture requires a "fine tuning" of m in function of η and γ to optimize $\overline{\mathbb{P}}_1^S$. On the other side, when the number of crystals is increased, the asymmetric architecture is always improving its performances. Values of $\overline{\mathbb{P}}_1^A$ close to the asymptotic ones, at least for experimentally available efficiencies, are reached already around eight crystals. This implies that, even if the expected energetic consumption for the AMHPS scheme is higher due to the implemented precompensation for the losses in the routing chain, the necessary overhead will be very limited. We believe that our results will be relevant to any future realization of the heralded single-photon source based on multiplexed architecture.

ACKNOWLEDGMENTS

The authors acknowledge the Strategic-Research-Project QUINTET of the Department of Information Engineering, University of Padova and the Strategic-Research-Project QUANTUMFUTURE of the University of Padova.

APPENDIX A: STATISTICS OF THE HERALDED SOURCES

We here provide a derivation of the MHPS statistics for the symmetric and asymmetric architecture with the number of crystals given by m. If we denote by $\tilde{\mu}_i$ the mean number of generated pairs from the ith crystal and with k_i the number of routers that the signal photon generated by the ith source needs to pass through, the asymmetric and symmetric architectures only differ from the expression of k_i and $\tilde{\mu}_i$: in the AMHPS, k_i is given by (7) and $\tilde{\mu}_i = \bar{\mu}/\gamma^{k_i}$, while for the SMHPS we have $k_i = k \equiv \log_2 m$ and $\tilde{\mu}_i = \tilde{\mu}/\gamma^k$, $\forall i$. We thus calculate the statistic of the output in this general framework.

The probability that the source i doesn't trigger is given by $p_i = e^{-\eta\tilde{\mu}_l}$. Let us denote by χ the first HS, starting from $i = 1$, that triggers. If no source triggers we set $\chi = 0$. The probability that $\chi = i$ is given by

$$\mathbb{P}(\chi = i) = \begin{cases} (1-p_i)\prod_{\ell=1}^{i-1} p_\ell, & \text{if} \quad i \neq 0, \\ \prod_{\ell=1}^{m} p_\ell & \text{if} \quad i = 0. \end{cases} = \begin{cases} (1-e^{-\eta\tilde{\mu}_i})e^{-\eta\sum_{\ell=1}^{i-1}\tilde{\mu}_\ell}, & \text{if} \quad i \neq 0, \\ e^{-\eta\sum_{\ell=1}^{m}\tilde{\mu}_\ell} & \text{if} \quad i = 0. \end{cases} \tag{A1}$$

The probability of having j photons in the ith signal channel (before the switches), provided that $\chi = i \neq 0$ is

$$\mathbb{P}(N_i = j|\chi = i) = \frac{\frac{\tilde{\mu}_i^j}{j!}e^{-\tilde{\mu}_i}(1-(1-\eta)^j)}{(1-e^{-\eta\tilde{\mu}_i})}, \quad \text{if} \quad i \neq 0, \tag{A2}$$

where N_i is the number of photons generated at the ith source. When $\chi = 0$ (no source triggers), the router will select the first source and the probability of having j photon on channel 1, provided that no sources have triggered is

$$\mathbb{P}(N_1 = j|\chi = 0) = \frac{\frac{\tilde{\mu}_i^j}{j!}e^{-\tilde{\mu}_i}(1-\eta)^j}{e^{-\eta\tilde{\mu}_i}}. \tag{A3}$$

The probability of having n photons in the final output provided that $\chi = i \neq 0$ and $N_i = j$ is given by

$$\mathbb{P}(\hat{N} = n|N_i = j, \chi = i) = \begin{cases} \binom{j}{n}(\gamma^{k_i})^n(1-\gamma^{k_i})^{j-n}, & \text{if} \quad i \neq 0 \quad \text{and} \quad n \leqslant j \\ 0 & \text{if} \quad i \neq 0 \quad \text{and} \quad n > j, \end{cases} \tag{A4}$$

while $\mathbb{P}(\hat{N} = n|N_1 = j, \chi = 0) = \binom{j}{n}(\gamma^{k_1})^n(1-\gamma^{k_1})^{j-n}$, if $n \leqslant j$. In the previous expression $\hat{N}$ is the number of photons generated at the global output.

Finally the probability of having n photons in the final output is given by

$$\begin{aligned} \mathbb{P}_n &= \sum_{j=n}^{\infty} \mathbb{P}(\hat{N} = n|N_1 = j, \chi = 0) \times \mathbb{P}(N_1 = j|\chi = 0)\mathbb{P}(\chi = 0) \\ &\quad + \sum_{i=1}^{m}\sum_{j=n}^{\infty} \mathbb{P}(\hat{N} = n|N_i = j, \chi = i)\mathbb{P}(N_i = j|\chi = i)\mathbb{P}(\chi = i) \\ &= \frac{[\tilde{\mu}_1\gamma^{k_1}(1-\eta)]^n e^{-\tilde{\mu}_1\gamma^{k_1}(1-\eta)}}{n!} e^{-\eta\sum_{\ell=1}^{m}\tilde{\mu}_\ell} + \sum_{i=1}^{m} \frac{(\tilde{\mu}_i\gamma^{k_i})^n e^{-\tilde{\mu}_i\gamma^{k_i}}}{n!}[1-(1-\eta)^n e^{-\eta(1-\gamma^{k_i})\tilde{\mu}_i}]e^{-\sum_{\ell=1}^{i-1}\eta\tilde{\mu}_\ell}. \end{aligned} \tag{A5}$$

Let us now specialize the last result for the symmetric case with $\tilde{\mu}_i = \bar{\mu}/\gamma^k$ and $k_i = k$. We obtain

$$\mathbb{P}_n^S = \frac{[\bar{\mu}(1-\eta)]^n e^{-\bar{\mu}(1-\eta)}}{n!} e^{-\eta\bar{\mu}\frac{2^k}{\gamma^k}} + \frac{\bar{\mu}^n e^{-\bar{\mu}}}{n!}\left[1-(1-\eta)^n e^{-\eta\bar{\mu}(\frac{1}{\gamma^k}-1)}\right]\sum_{i=1}^{m} e^{-(i-1)\eta\frac{\bar{\mu}}{\gamma^k}}, \tag{A6}$$

and performing the last sum we obtain (6).

In the asymmetric case we have $\tilde{\mu}_i = \tilde{\mu}/\gamma^{k_i}$ and the k_i are given by (7). We obtain

$$\mathbb{P}_n^A = \frac{[\tilde{\mu}(1-\eta)]^n e^{-\tilde{\mu}(1-\eta)}}{n!} e^{-\eta\tilde{\mu}(\frac{1}{\gamma^{m-1}}+\sum_{\ell=1}^{m-1}\frac{1}{\gamma^\ell})} + \frac{\tilde{\mu}^n e^{-\tilde{\mu}}}{n!}\sum_{i=1}^{m}\left[1-(1-\eta)^n e^{-\eta\tilde{\mu}(\frac{1}{\gamma^{k_i}}-1)}\right] e^{-\eta\tilde{\mu}_\ell\sum_{\ell=1}^{i-1}\frac{1}{\gamma^\ell}}, \tag{A7}$$

and performing the sum on the exponents we obtain (9).

Note that, by using in $\mathbb{P}_n^A$ or $\mathbb{P}_n^S$ perfect efficiency $\eta = 1$ and perfect transmission $\gamma = 1$, we get the probability outputs of perfect MHPS, Eq. (3).

APPENDIX B: ANALYSIS OF THE TWO-CRYSTAL ARCHITECTURE: SYMMETRY IS NOT OPTIMAL

In this section we will prove that the (ideal) two-crystal architecture where the two crystals are driven with the same pump laser intensity represents a suboptimal choice for the one-photon probability. We here consider a MHPS composed by two crystals each one fed with different intensities such that the mean number of emitted pairs are μ_1 and μ_2, respectively. The probability of having n photons in the output is obtained from Eq. (A5) by using $m = 2$, $\gamma = 1$, and $\eta = 1$:

$$\mathbb{P}_n = \delta_n e^{-\mu_1-\mu_2} + (1-\delta_n)\left(\frac{\mu_1^n e^{-\mu_1}}{n!} + \frac{\mu_2^n e^{-\mu_1-\mu_2}}{n!}\right). \tag{B1}$$

In particular, the probability of having one photon in the final output is given by

$$\mathbb{P}_1 = \mu_1 e^{-\mu_1} + \mu_2 e^{-(\mu_1+\mu_2)}, \tag{B2}$$

and its maximum is achieved when

$$(\mu_1, \mu_2) = (1-e^{-1}, 1). \tag{B3}$$

This can be seen in Fig. 10 where the contours of $\mathbb{P}_1$ are plotted: the blue line represents the cases $\mu_2 = \mu_1$. Also by using the performance parameter introduced in Sec. II B it is straightforward to show that by using $\mu_1 \neq \mu_2$ leads to better performances with respect to the choice $\mu_1 = \mu_2$.

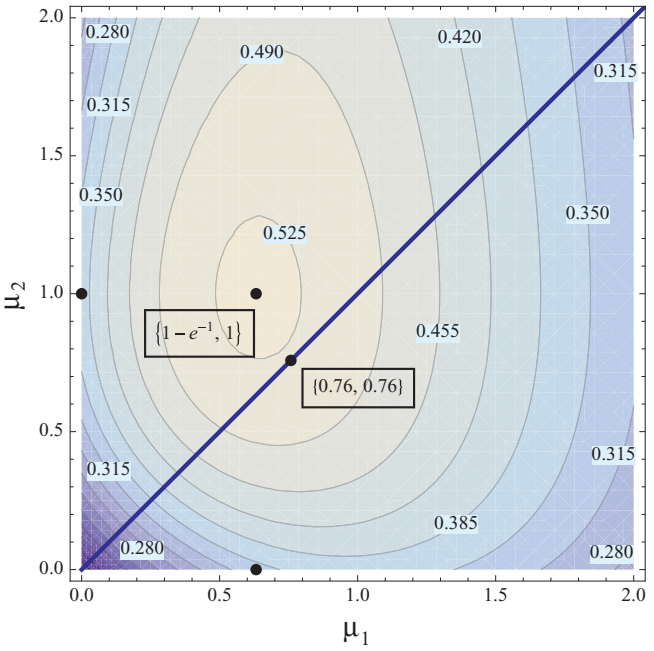

FIG. 10. (Color online) Contours of the one-photon probability (B2) for the two crystals MHPS. The blue line represents the $\mu_1 = \mu_2$ case.

Therefore, we conclude that, in general, feeding all the crystals with the same laser intensities, leads to suboptimal performances. It is worth noticing that the asymmetry comes from the switch selection: The first source is initially checked and, only if this source doesn't trigger, the switch considers the second source. As we demonstrated, this asymmetry can be exploited to improve the probability of having one photon at the output channel.

In the ideal case (perfect detection and transmission), it is straightforward to compute the intensities that lead to the one-photon probability optimal value generalizing the analysis above. Anyway, such optimization task become quite nontrivial if finite efficiency are taken into account, especially for a large number of crystals.

APPENDIX C: INFINITE CRYSTALS LIMIT OF THE SMHPS

We here analytically show that the one-photon probability of the symmetric scheme approaches the one-photon probability of the faint laser when the pump intensities are chosen in order to have the same SNR. The SNR of the SHMPS is

$$\frac{\tilde{\mu}\left[1-e^{-\frac{\eta\tilde{\mu}}{\gamma^k}}e^{\eta\tilde{\mu}}(1-\eta) - e^{-\frac{2^k}{\gamma^k}\eta\tilde{\mu}}(1-e^{\eta\tilde{\mu}}(1-\eta))\right]}{e^{\tilde{\mu}} - 1 - \tilde{\mu} - e^{-\frac{\eta\tilde{\mu}}{\gamma^k}}[(e^{\tilde{\mu}} - e^{\eta\tilde{\mu}}(1+\tilde{\mu}-\eta\tilde{\mu})] + e^{-\frac{2^k}{\gamma^k}\eta\tilde{\mu}}[(1+\tilde{\mu}) - e^{\eta\tilde{\mu}}(1+\tilde{\mu}-\eta\tilde{\mu})]}. \tag{C1}$$

In the large k limit, when $\gamma \neq 1$, the previous expression is equal to the SNR of the faint laser, namely $\frac{\tilde{\mu}}{e^{\tilde{\mu}}-1-\tilde{\mu}}$. When $\tilde{\mu} = \mu$, the SNRs are equal in the large k limit and the one-photon probability of the SHMPS becomes

$$\mathbb{P}_1^S = \mu e^{-\mu}\frac{1-e^{-\frac{\eta\mu}{\gamma^k}}e^{\eta\mu}(1-\eta) - e^{-\frac{2^k}{\gamma^k}\eta\mu}[1-e^{\eta\mu}(1-\eta)]}{1-e^{-\frac{\eta\mu}{\gamma^k}}} \sim \mu e^{-\mu} \quad \text{for } k\to\infty \text{ and } \gamma \neq 1\,, \tag{C2}$$

asymptotic, in the large number of crystal limit, to the one-photon probability of the faint laser.

[1] A. Politi, M. J. Cryan, J. G. Rarity, S. Yu, and J. L. O'Brien, Science **320**, 646 (2008).
[2] J. Matthews, A. Politi, A. Stefanov, and J. O'Brien, Nature Photonics **3**, 346 (2009).
[3] L. Sansoni, F. Sciarrino, G. Vallone, P. Mataloni, A. Crespi, R. Ramponi, and R. Osellame, Phys. Rev. Lett. **105**, 200503 (2010).
[4] A. Crespi, R. Ramponi, R. Osellame, L. Sansoni, I. Bongioanni, F. Sciarrino, G. Vallone, and P. Mataloni, Nature communications **2**, 566 (2011).
[5] E. Knill, R. Laflamme, and G. J. Milburn, Nature (London) **409**, 46 (2001).
[6] V. Scarani *et al*., Rev. Mod. Phys. **81**, 1301 (2009).
[7] M. Canale *et al*., in *Proceedings of the 4th International Symposium on Applied Sciences in Biomedical and Communication Technologies, ISABEL'11* (ACM, New York, 2011), pp. 1–5.
[8] D. Bacco *et al*. (unpublished).
[9] P. Villoresi *et al*., New J. Phys. **10**, 033038 (2008).
[10] I. Capraro, A. Tomaello, A. Dall'Arche, F. Gerlin, R. Ursin, G. Vallone, and P. Villoresi, Phys. Rev. Lett. **109**, 200502 (2012).
[11] W.-Y. Hwang, Phys. Rev. Lett. **91**, 057901 (2003).
[12] X. Ma, B. Qi, Y. Zhao, and H.-K. Lo, Phys. Rev. A **72**, 012326 (2005).
[13] G. Brassard, N. Lütkenhaus, T. Mor, and B. C. Sanders, Phys. Rev. Lett. **85**, 1330 (2000).
[14] S. Ramelow, A. Mech, M. Giustina, S. Groeblacher, W. Wieczorek, A. Lita, B. Calkins, T. Gerrits, S. W. Nam, A. Zeilinger, and R. Ursin, arXiv:1211.5059.
[15] A. L. Migdall, D. Branning, and S. Castelletto, Phys. Rev. A **66**, 053805 (2002).
[16] J. H. Shapiro and F. N. Wong, Opt. Lett. **32**, 2698 (2007).
[17] X.-s. Ma, S. Zotter, J. Kofler, T. Jennewein, and A. Zeilinger, Phys. Rev. A **83**, 043814 (2011).
[18] A. Christ and C. Silberhorn, Phys. Rev. A **85**, 023829 (2012).
[19] S. Tanzilli, A. Martin, F. Kaiser, M. De Micheli, O. Alibart, and D. Ostrowsky, Laser & Photonics Reviews **6**, 115 (2012).
[20] X. Caillet, A. Orieux, A. Lemaître, P. Filloux, I. Favero, G. Leo, and S. Ducci, Opt. Express **18**, 9967 (2010).
[21] E. Pomarico, B. Sanguinetti, T. Guerreiro, R. Thew, and H. Zbinden, Optics Express **20**, 23846 (2012).
[22] D. H. Smith, G. Gillett, M. P. de Almeida, C. Branciard, A. Fedrizzi, T. J. Weinhold, A. Lita, B. Calkins, T. Gerrits, H. M. Wiseman, S. W. Nam, and A. G. White, Nat. Comm. **3**, 625 (2012).
[23] M. D. Eisaman, J. Fan, A. Migdall, and S. V. Polyakov, Rev. Sci. Instrum. **82**, 071101 (2011).
[24] P. Dong, S. Liao, H. Liang, R. Shafiiha, D. Feng, G. Li, X. Zheng, A. V. Krishnamoorthy, and M. Asghari, Opt. Express **18**, 25225 (2010).
[25] G. T. Reed, G. Mashanovich, F. Y. Gardes, and D. J. Thomson, Nature Photonics **4**, 518 (2010).